Computer Assisted Mechanics and Engineering Sciences, **10**: 265–281, 2003.

Discussion on application of piece-wise linear weight functions in 2D contact problems

Marek Klisiński, Chouping Luo and Eligiusz Postek
Division of Structural Mechanics, Luleå University of Technology
SE-971 87 Luleå, Sweden

(Received August 16, 2001)

Standard higher order finite elements often perform unsatisfactory in contact problems. The major difficulties are caused by uneven distribution of nodal forces resulting in oscillating contact pressures. The paper presents a new approach that eliminates this drawback. The weight functions are chosen in such a way that even distributions of nodal forces are obtained. It is achieved by applying piece-wise linear functions. Two new 2D isoparametric quadratic elements are derived: 6-node triangle and 8-node quadrilateral, and tested in many examples. The new elements have unsymmetric stiffness matrices, but the provided examples show their good performance in contact problems.

1. Introduction

Contact problems are common in many engineering applications and a lot of progress has been achieved during recent years (see e.g. [3] for additional references). However, it seems that standard higher order elements experience difficulties in many rather simple cases (see e.g. [5]). One possible explanation of these problems is that the resulting nodal forces are unevenly distributed giving oscillating pressures. In extreme cases can even tensile forces appear whereas in reality contact pressure occurs. In the general purpose finite element program ABAQUS the 6-node triangular finite element CPS6M gives smooth nodal force distributions, but it is patented and no information is available about its design [1]. The present study follows the same line of reasoning and examines possibilities to obtain even pressure distributions by modification of weight functions.

In solving a problem by applying FE method, the weight functions play an important role. They sometimes decide how good or accurate results will be achieved. The weight functions can be defined in different ways leading to diverse methods, such as the point collocation method, the subdomain collocation method, the least-squares method, or the Galerkin method, etc. (see e.g. [9]). Accuracy of each method depends severely on problems solved. The Galerkin method is most popular when solving elliptic equations and results in symmetric stiffness and mass matrices which leads to lower computational costs. However, other weight functions are also used when required. For example, exponential weight functions are employed when considering incompressible gas liquid flow in [10]. In this paper the major focus is on contact problems, either static or dynamic, by using quadratic elements. The standard elements constructed according to the Galerkin method result in uneven normal pressures and tangential shear stresses along the contact area. As shown in examples, it can be concluded that the values of contact forces at corner nodes are around half of those at midside nodes.

In this paper a new weighted residual method for 2-D frictional contact problems is proposed. The starting point of this new method is to make use of piece-wise linear weight functions and quadratic shape functions to establish FE formulations. An obvious implication is that the stiffness and mass matrices will not be symmetric. Therefore, from the theoretical point of view the proposed formulation is more expensive than the Galerkin method. However, in many formulations considering

friction (see e.g. [3, 11]) the resulting matrices are unsymmetric anyway so in practice this drawback may not matter at all. In any case, if the results turn out to be more accurate, the extra consumed time will be well spent.

Many examples will be presented further in the paper. The first one explains how the method works compared to the Galerkin method in a simple structure consisting of two elements. Several other examples show the performance and efficiency of the developed new method in 2-D contact problems.

2. Weak formulation

For 2-D problems, the displacements, strains, stresses, tractions and body forces do not depend on z-coordinate. In this paper problems under plane stress, plane strain and axisymmetric conditions are considered. The basic differential equations of motion, including dynamic loads but without damping, can be written in matrix notation as

$$\tilde{\nabla}^T \mathbf{s} + \rho \ddot{\mathbf{u}} + \mathbf{b} = 0, \tag{1}$$

where

$$\tilde{\nabla}^T = \begin{bmatrix} \dfrac{\partial}{\partial x} & 0 & \dfrac{\partial}{\partial y} \\ 0 & \dfrac{\partial}{\partial y} & \dfrac{\partial}{\partial x} \end{bmatrix}$$ is the matrix differential operator, $\mathbf{s} = [\sigma_{xx}\ \sigma_{yy}\ \sigma_{xy}]^T$ is the stress vector,

ρ is the material density, $\mathbf{u} = [u_x\ u_y]^T$ is the displacement vector and $\ddot{\mathbf{u}} = \partial^2\mathbf{u}/\partial t^2$, whereas $\mathbf{b} = [b_x\ b_y]^T$ is the body force vector.

The corresponding weak formulation of a 2-D problem is

$$\int_A \left(\tilde{\nabla}\mathbf{v}\right)^T \mathbf{s}\, t\, dA + \int_A \mathbf{v}^T \ddot{\mathbf{u}} \rho\, t\, dA = \int_\Gamma \mathbf{v}^T \mathbf{t}\, t\, d\Gamma + \int_A \mathbf{v}^T \mathbf{b}\, t\, dA, \tag{2}$$

where $\mathbf{v}$ is the virtual displacement vector, A is an area of interest of thickness $t(x, y)$ with boundary Γ and $\mathbf{t} = [t_x, t_y]^T$ is the traction vector.

The displacement vector $\mathbf{u}$ is approximated by

$$\mathbf{u} = \mathbf{N}\mathbf{a} \tag{3}$$

in which $\mathbf{N}$ is the shape function matrix and $\mathbf{a}$ is the vector containing displacements at nodes, so

$$\ddot{\mathbf{u}} = \mathbf{N}\ddot{\mathbf{a}}. \tag{4}$$

Assuming small deformations and plane stress or plane strain conditions, the strain vector $\mathbf{e} = [\varepsilon_{xx}\ \varepsilon_{yy}\ \Gamma_{xy}]^T$ is derived from the displacements using the kinematic relation

$$\mathbf{e} = \tilde{\nabla}\mathbf{u}. \tag{5}$$

Therefore, defining $\mathbf{B} = \tilde{\nabla}\mathbf{N}$, the stress vector for an elastic problem takes the form

$$\mathbf{s} = \mathbf{D}\mathbf{B}\mathbf{a}, \tag{6}$$

where $\mathbf{D}$ is the constitutive matrix.

Let us express the virtual displacement vector with help of weight functions as

$$\mathbf{v} = \mathbf{W}\mathbf{c}, \tag{7}$$

where $\mathbf{W}$ is the matrix of weight functions and $\mathbf{c}$ an arbitrary vector of the same size as $\mathbf{a}$.

Defining

$$\overline{\mathbf{B}} = \widetilde{\nabla}\mathbf{W} \tag{8}$$

and substituting Eqs. (4), (6) and (7) into Eq. (2) results in the FE method equation

$$\mathbf{M}\ddot{\mathbf{a}} + \mathbf{K}\mathbf{a} = \mathbf{f}, \tag{9}$$

where

$$\mathbf{K} = \int_A \overline{\mathbf{B}}^T \mathbf{D}\mathbf{B}\, t\, dA \tag{10}$$

is the stiffness matrix,

$$\mathbf{M} = \int_A \mathbf{W}^T \mathbf{N} \rho\, t\, dA \tag{11}$$

is the mass matrix and

$$\mathbf{f} = \int_\Gamma \mathbf{W}^T \mathbf{t}\, t\, d\Gamma + \int_A \mathbf{W}^T \mathbf{b}\, t\, dA \tag{12}$$

is the force vector.

Let us consider the natural frequencies of vibration, i.e without external forces, $\mathbf{f} = \mathbf{0}$. Each displacement executes harmonic motion in phase with all other displacements. Therefore

$$\begin{aligned} \mathbf{a} &= \overline{\mathbf{a}} \sin \omega t, \\ \ddot{\mathbf{a}} &= -\omega^2 \overline{\mathbf{a}} \sin \omega t, \end{aligned} \tag{13}$$

where $\overline{\mathbf{a}}$ is the amplitude of nodal displacements and ω is the natural circular frequency. Equations (9) and (13) yield the following eigenvalue problem

$$(\mathbf{K} - \omega^2 \mathbf{M})\overline{\mathbf{a}} = \mathbf{0}. \tag{14}$$

Matrix $\overline{\mathbf{B}}$ depends on which method is adopted to define weight functions. If weight functions are taken the same as shape functions, that is, Galerkin method is applied, $\mathbf{W} = \mathbf{N}$ and $\overline{\mathbf{B}} = \mathbf{B}$. This paper proposes another method to define weight functions for 2-D triangular and quadratic elements concerning contact problems, which thereby leads to a new way to calculate stiffness and mass matrices.

3. Derivation of weight functions

The basic characteristic of the method is to use weight functions which are piece-wise linear over the element while shape functions are kept quadratic as in the standard formulation. Let us start from a 6-node isoparametric triangular element, shown in Fig. 1 in the parent domain, to describe the principles of the method in deriving the weight functions.

In the element shown in Fig. 1, node 1 is at the origin of the coordinate system. Line segments 1-2 and 1-3 are along x- and y-axis, respectively, and have unit lengths. Nodal point 4, 5 and 6 are located at the middle points of line segments 1-2, 2-3 and 3-1 respectively. The element consists of four subelements: A_1, A_2, A_3 and A_4.

The explanation about how the weight functions are defined in the method is presented in Fig. 2, in which weight functions of nodes 1 and 4 in the 6-node triangular element are shown.

As Fig. 2 shows the weight functions are created according to the following principles: 1) The weight function of a node is non-zero only over the adjoining subelements to the corresponding

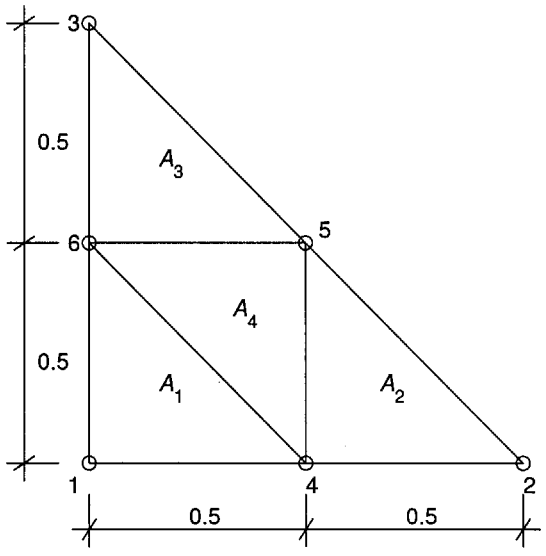

Fig. 1. 6-node isoparametric triangular element in parent domain

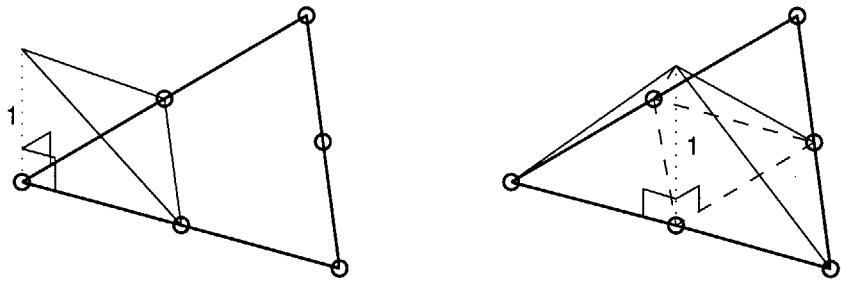

Fig. 2. Weight functions of node 1 and node 4

node in the triangular element, for example, w_1, weight function for node 1, is non-zero only over the subelement A_1; 2) The weight function of a node is linear over its non-zero domain; 3) The weight functions must be continuous over the element; 4) The value of a weight function is 1 at the corresponding node and 0 at all the other nodes. According to these principles six weight functions for every node in the triangular element are defined as

$$\begin{cases} w_1 = 1 - 2x - 2y & \text{in } A_1, \\ w_1 = 0 & \text{in } A_2,\ A_2,\ A_4; \end{cases} \tag{15}$$

$$\begin{cases} w_2 = 2x - 1 & \text{in } A_2, \\ w_2 = 0 & \text{in } A_1,\ A_3,\ A_4; \end{cases} \tag{16}$$

$$\begin{cases} w_3 = 2y - 1 & \text{in } A_3, \\ w_3 = 0 & \text{in } A_1,\ A_2,\ A_4; \end{cases} \tag{17}$$

$$\begin{cases} w_4 = 2x & \text{in } A_1, \\ w_4 = 2 - 2x - 2y & \text{in } A_2, \\ w_4 = 0 & \text{in } A_3, \\ w_4 = 1 - 2y & \text{in } A_4; \end{cases} \tag{18}$$

$$\begin{cases} w_5 = 0 & \text{in } A_1, \\ w_5 = 2y & \text{in } A_2, \\ w_5 = 2x & \text{in } A_3, \\ w_5 = 2x + 2y - 1 & \text{in } A_4; \end{cases} \tag{19}$$

$$\begin{cases} w_6 = 2y & \text{in } A_1, \\ w_6 = 0 & \text{in } A_2, \\ w_6 = 2 - 2x - 2y & \text{in } A_3, \\ w_6 = 1 - 2x & \text{in } A_4. \end{cases} \tag{20}$$

4. Stiffness matrix

The stiffness matrix is expressed by Eq. (10). The element stiffness matrix $\mathbf{K}^e$ for a 6-node triangular element can be calculated by a similar formula

$$\mathbf{K}^e = \int_{A^e} \overline{\mathbf{B}}^T \mathbf{D} \mathbf{B}\, t\, dA \tag{21}$$

in which A^e is the area of the triangular element, t is the thickness of the element, and assuming isotropic linear elasticity the constitutive matrix is expressed by

$$\mathbf{D} = \frac{E}{1-\nu^2} \begin{bmatrix} 1 & \nu & 0 \\ \nu & 1 & 0 \\ 0 & 0 & \frac{1}{2}(1-\nu) \end{bmatrix}, \tag{22}$$

where E is the Young modulus and ν is the Poisson ratio.

$\mathbf{B}$ matrix contains derivatives of the standard quadratic shape functions, whereas $\overline{\mathbf{B}}$ contains the derivatives of the weight functions Eqs. (15)–(20). However, since the derivatives of weight functions are not continuous over all the element, but constant within each subelement, the numerical integration should be performed over each subelement and the results added together according to

$$\mathbf{K}^e = \sum_{i=1}^{4} \int_{A_1} \overline{\mathbf{B}}_i^T \mathbf{D} \mathbf{B}\, t\, dA_i, \tag{23}$$

where $\overline{\mathbf{B}}_i$ is $\overline{\mathbf{B}}$ in the corresponding integration domain A_i. It is obvious that the stiffness matrix $\mathbf{K}^e$ derived by this method is unsymmetric.

The mass matrix $\mathbf{M}^e$ can be derived in the same manner as the stiffness matrix.

5. 8-node quadrilateral element

The weight functions for a 8-node quadrilateral element could be derived in a similar way as for the 6-node triangular element. However, in this paper the main focus is on the discussion of the merits of the derived 6-node triangular element. Therefore, the stiffness and mass matrices for a 8-node quadrilateral element will be set up from the matrices of two 6-node triangular elements. The procedures could be completed as follows: firstly, build a 9-node structure which consists of two 6-node triangular elements, as shown in the left side of Fig. 3; and then remove internal D.O.F. by *static condensation* in the linear static problem or by *Guyan* reduction in the eigenvalue problem [4], resulting in an 8-node quadrilateral element shown at the right side of Fig. 3.

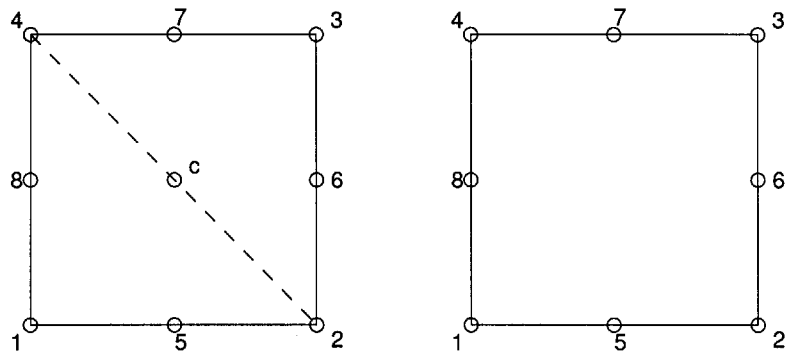

Fig. 3. Creation of 8-node quadrilateral element

6. Initial stress matrix

Initial stress matrix $\mathbf{K}_\sigma$ is usually developed to calculate critical load of a structure. By solving

$$(\mathbf{K} + \lambda \mathbf{K}_\sigma)\tilde{\mathbf{d}} = 0, \tag{24}$$

where $\tilde{\mathbf{d}}$ is the displacement vector identifying the buckled shape, but not its magnitude, the critical (buckling) load is associated with λ_{cr}, the lowest magnitude eigenvalue of Eq. (24).

The derivation of initial stress matrix is described in detail in e.g. [2] or [7]. However, since this paper focus on new weight functions for 2D triangular and quadratic elements, the derivation of initial stiffness matrix must be modified in the same way as the derivation of stiffness and mass matrices was. Therefore, the initial stress matrix can be expressed by

$$\mathbf{K}_\sigma = \int_A \overline{\mathbf{G}}^T \mathbf{S} \mathbf{G}\, t\, dA, \tag{25}$$

where $\mathbf{G}$ and $\mathbf{S}$ matrices are calculated in the usual way, while $\overline{\mathbf{G}}$ is modified as follows

$$\overline{\mathbf{G}} = \begin{bmatrix} \frac{dw_1}{dx} & 0 & \dots & \frac{dw_n}{dx} & 0 \\ \frac{dw_1}{dy} & 0 & \dots & \frac{dw_n}{dy} & 0 \\ 0 & \frac{dw_1}{dx} & \dots & 0 & \frac{dw_n}{dx} \\ 0 & \frac{dw_1}{dy} & \dots & 0 & \frac{dw_n}{dy} \end{bmatrix} \tag{26}$$

and n is the number of nodes.

7. Numerical examples

In this section a simple example will be presented first to explain how this method works in comparison with the Galerkin method and then more numerical examples will be investigated to explore the properties of the method developed in application to contact problems. The algorithm has been performed by inserting a user subroutine into the general purpose finite element program ABAQUS. The user subroutine calculates element stiffness and mass matrices based on the described method, the right hand side force vector as well as stresses and strains at the integration points. For the purpose of comparison the corresponding results either from standard ABAQUS element or from reference papers are also presented.

7.1. Simple structure with two elements

Let us present a simple example, which explains how the method works. The structure in Fig. 4 is taken into account. It is a square with unit side length and thickness. It endures unit distributed load on its upper side and is constrained on the y-direction along its lower side. It is meshed into two 6-node triangular elements with 9 nodes altogether.

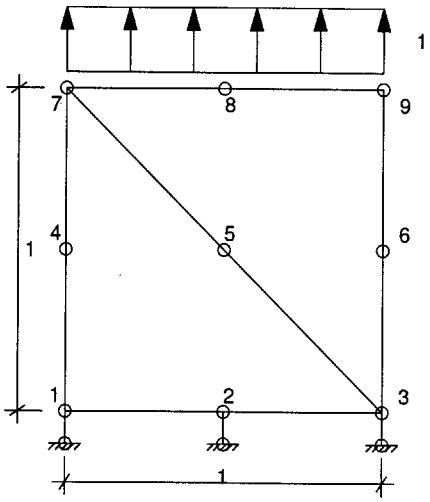

Fig. 4. The simple structure with two triangular elements

The results concerning reaction forces at contact nodes are given in Fig. 5 for the weight functions based on the new method and on the Galerkin method, respectively. On the right side of Fig. 5, which shows the results from the Galerkin method, the reaction force at central node is four times larger than the reactions at the other two nodal points. Therefore, if there are more than two elements located along the contact surface (in real analysis this is always the case), the values at corner nodes will be half the size as those of those at midside nodes. That is, the contact reaction forces obtained from the Galerkin method are nor evenly distributed along the contact surface. In fact the distribution of contact forces has a sawtooth shape. On the contrary the new method will lead to even distributions, which is reasonable, as shown on the left side of Fig. 5.

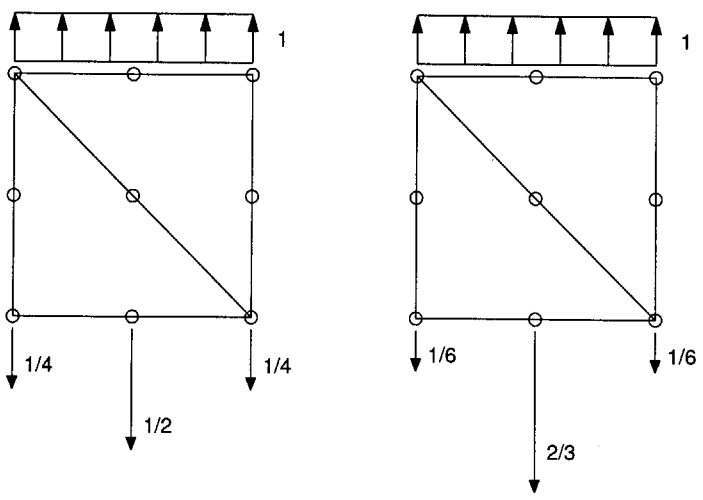

Fig. 5. The contact force calculated from the new method and the Galerkin method

7.2. Elastic block on a rigid surface

This example was, for the first time, presented by Oden and Pires [8]. Wriggers *et al.* have also used this example in [11]. The problem considers an elastic block pressed against a rigid surface and at the same time pulled by a tangential force uniformly distributed along its right lateral side as shown in Fig. 6. As in the original example friction is not present for the first and last elements in the contact area, i.e. perfectly smooth boundary condition is assumed under these two elements. Young's modulus E, Poisson's ratio ν and the coefficient of friction are taken equal to 1000 per length square, 0.3 and 0.3, respectively.

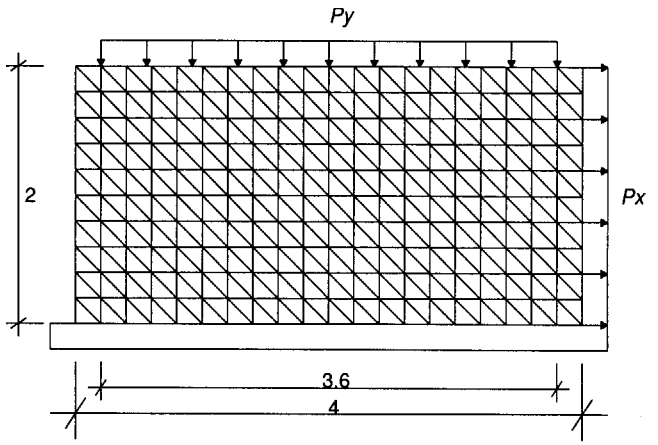

Fig. 6. The elastic block on a rigid foundation

The example has been analysed by two kinds of elements: 6-node triangular element and 8-node quadrilateral element. The latter is derived by condensing two 6-node triangular elements as explained in the previous section. The standard ABAQUS elements adopted to make a comparison with 6-node triangular element are CPS6 and CPS6M whereas CPS8 is used to compare with 8-node quadrilateral element. The elastic block is meshed with 400 6-node triangular elements and with 200 8-node quadrilateral elements, respectively.

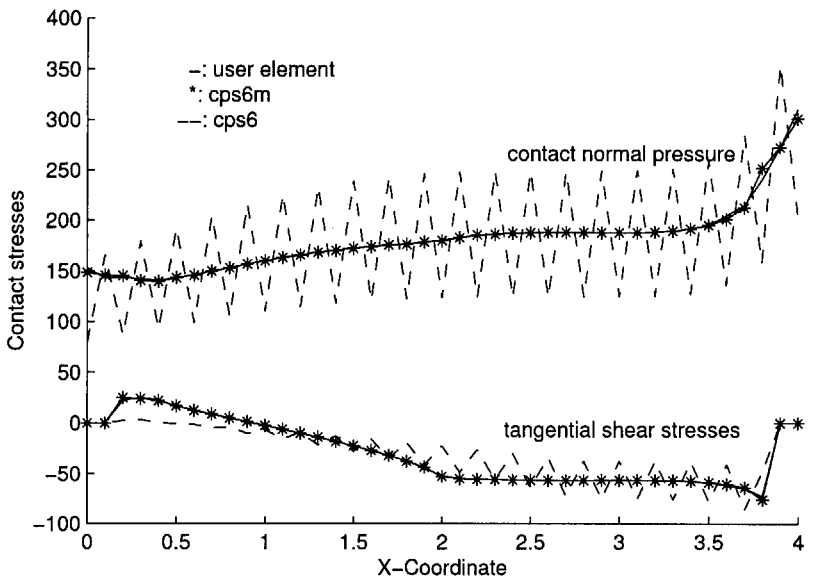

Fig. 7. Stresses along the contact area calculated with 6-node triangular elements

Figures 7 and 8 give comparison of contact stresses. For CPS6 and CPS8, both contact normal pressure and tangential shear stresses look like a sawtooth. The results based on the user defined element according the method fit with those obtained from CPS6M very well.

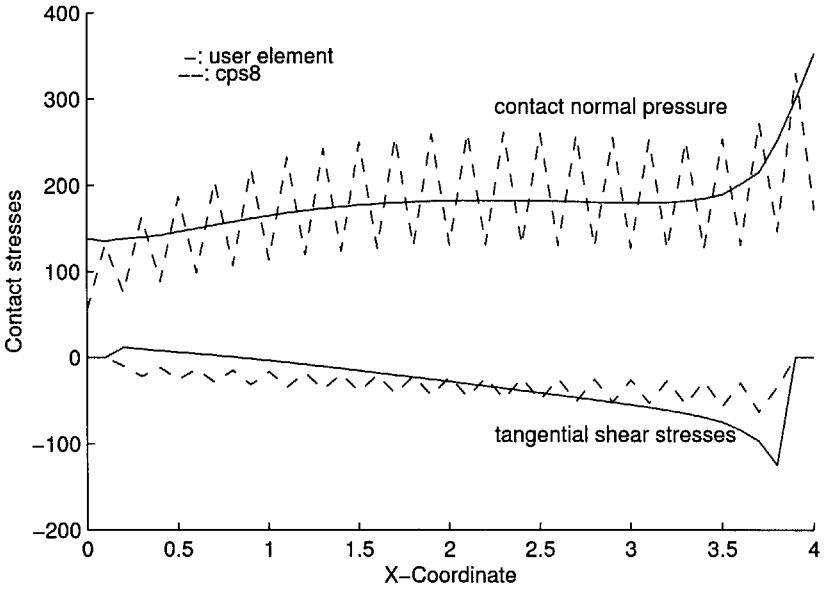

Fig. 8. Stresses along the contact area calculated with 8-node quadrilateral elements

7.3. Contact of an elastic body and a parabolic rigid punch

This example also originates from Oden and Pires [8]. In this example, an elastic body is indented by a parabolic rigid punch and subjected to applied normal tractions $\mathbf{t}$, as shown in Fig. 9. Young's modulus, Poisson's ration and the coefficient of friction are taken equal to 1000 (non-dimensional units), 0.25 and 0.6 respectively.

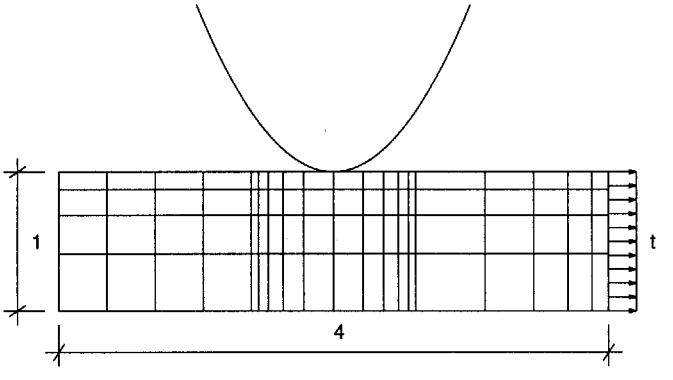

Fig. 9. Indentation of an elastic body, subjected to normal traction, by a parabolic rigid punch

For the purpose of comparison with results of Oden and Pires [8], the elastic body is meshed in the same way. The mesh consists of 76 8-node quadrilateral element. The normal force, which is defined to cause an indentation of depth $d = 0.25$, is approximately 215. The applied total tangential force is 10% of the normal force. The stresses on the contact area from Oden and Pires, standard element CPS8 and from user element are given in Fig. 10.

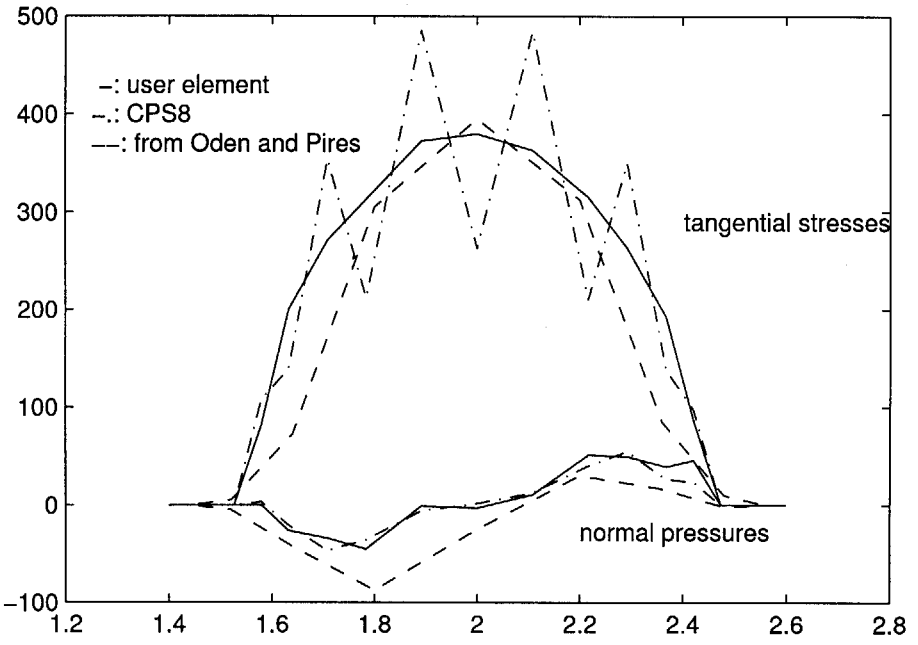

Fig. 10. Stresses distribution along the contact area

7.4. Rigid punch acting on an elastic body

This example is adopted to check reaction forces along the contact surface. The problem was studied by Jarzębowski and Maciejewski [5]. The dimensions and mesh of the elastic body are shown in Fig. 11. The body is constrained on its both lateral sides and on the lower side. The plate is placed at the centre of the elastic body's upper side. The mesh is constructed in such a way that smallest elements are exactly under the rigid plate and the elements along the edges have the largest possible dimension. Young's modulus, Poisson's ration and the friction angle are taken equal to $1.2 \cdot 10^8$ per length square, 0.25 and 20, respectively. Unit thickness is assumed. The applied pressing force is 40 kN.

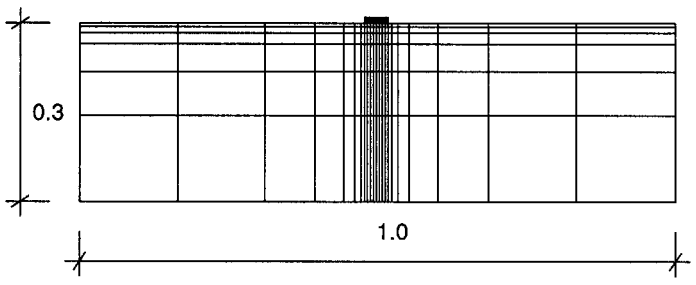

Fig. 11. Profile and mesh of the elastic body

Jarzębowski and Maciejewski pointed out that the 8-node element predicted erroneous distributions of nodal forces and should be avoided in the case of contact problem [5]. However in our study, the 8-node rectangular element created by the method gives satisfactory results in this contact problem. Results from ABAQUS standard element CPS8 and from user element are presented in Figs. 12–14.

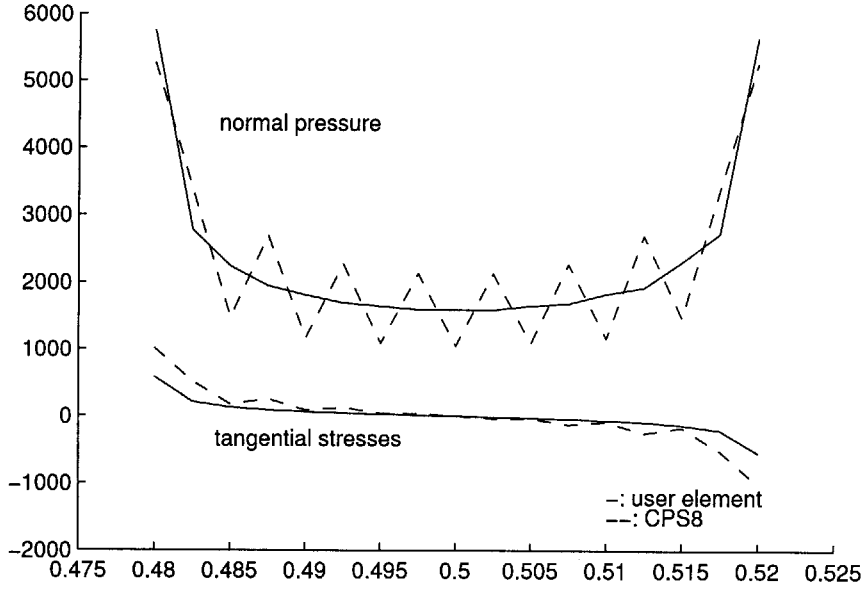

Fig. 12. Stresses distribution along the contact area

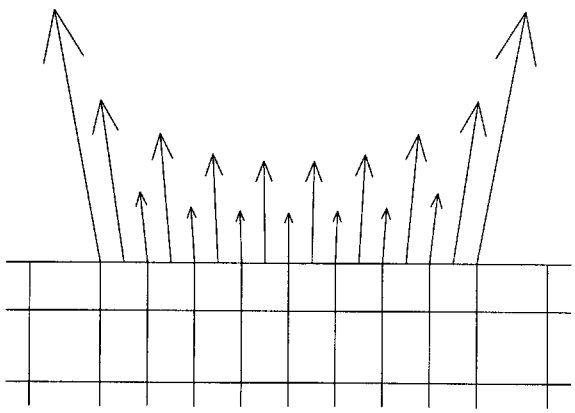

Fig. 13. Reaction forces along the contact area using CPS8

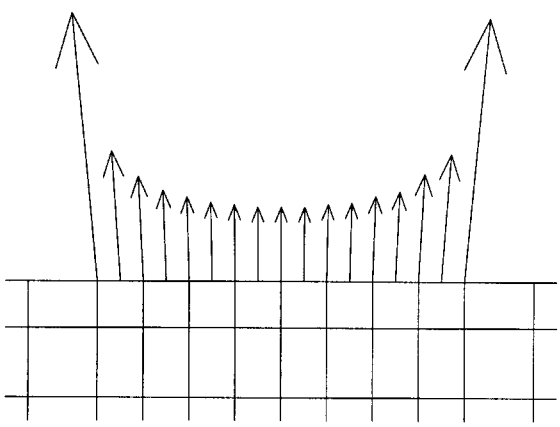

Fig. 14. Reaction forces along the contact area from user element

7.5. Contact of a changing cross-section column and rigid surfaces

In this example a changing cross-section column which can be created by rotating the section, shown in Fig. 15, around axis ab is considered. The column has four surfaces contacting with rigid surfaces. Young's modulus, Poisson's ratio and the coefficient of friction are taken equal to $2.1 \cdot 10^8$ kN per length square, 0.3 and 0.3, respectively. The density of the column is taken the same as that of steel, 7856 kg/m^3. The pressing load is applied in such a way that the downward displacement of the contact surface 4 is equal to 1 mm.

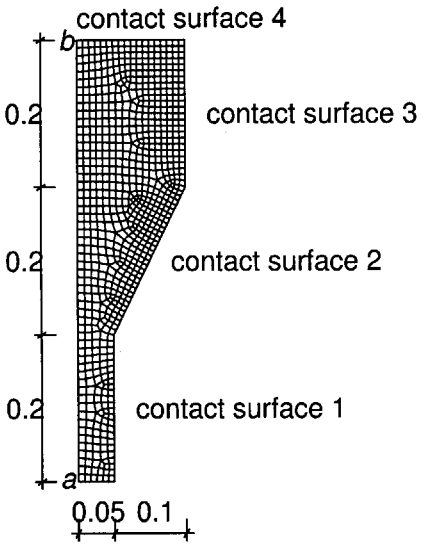

Fig. 15. Profile and mesh of the section

The mesh of the section consists of 759 8-node axisymmetric elements. The section is constrained along the axis of rotation in the horizontal direction. The results in form of contact stresses along every contact surface are given in Figs. 16–23.

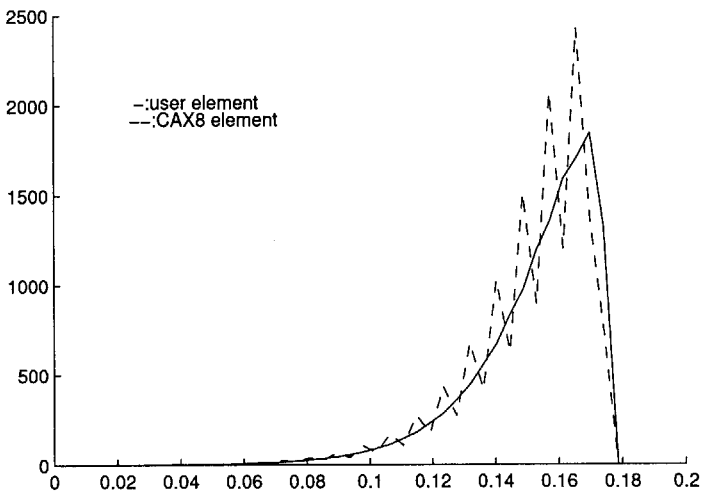

Fig. 16. Normal pressures along contact surface 1

Application of this method in dynamics has been also checked in this example. Table 1 gives the first six eigenvalues calculated by using different elements. As Table 1 shows, the method developed

7.5. Contact of a changing cross-section column and rigid surfaces

In this example a changing cross-section column which can be created by rotating the section, shown in Fig. 15, around axis *ab* is considered. The column has four surfaces contacting with rigid surfaces. Young's modulus, Poisson's ratio and the coefficient of friction are taken equal to $2.1 \cdot 10^8$ kN per length square, 0.3 and 0.3, respectively. The density of the column is taken the same as that of steel, 7856 kg/m^3. The pressing load is applied in such a way that the downward displacement of the contact surface 4 is equal to 1 mm.

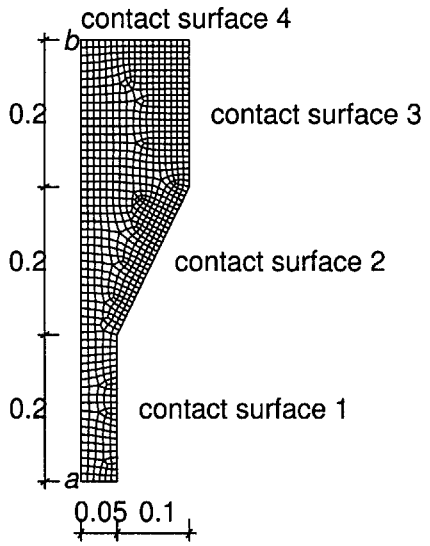

Fig. 15. Profile and mesh of the section

The mesh of the section consists of 759 8-node axisymmetric elements. The section is constrained along the axis of rotation in the horizontal direction. The results in form of contact stresses along every contact surface are given in Figs. 16–23.

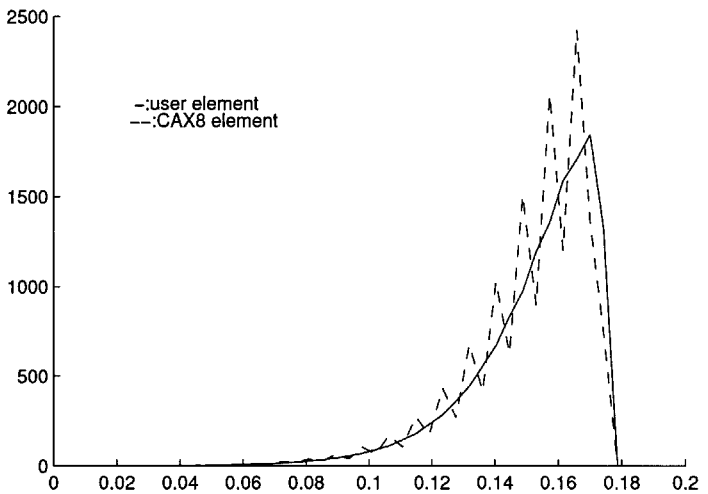

Fig. 16. Normal pressures along contact surface 1

Application of this method in dynamics has been also checked in this example. Table 1 gives the first six eigenvalues calculated by using different elements. As Table 1 shows, the method developed

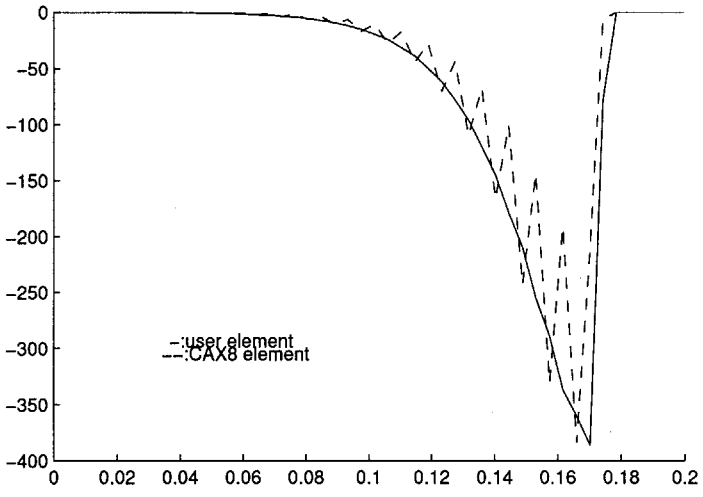

Fig. 17. Tangential shear stresses along contact surface 1

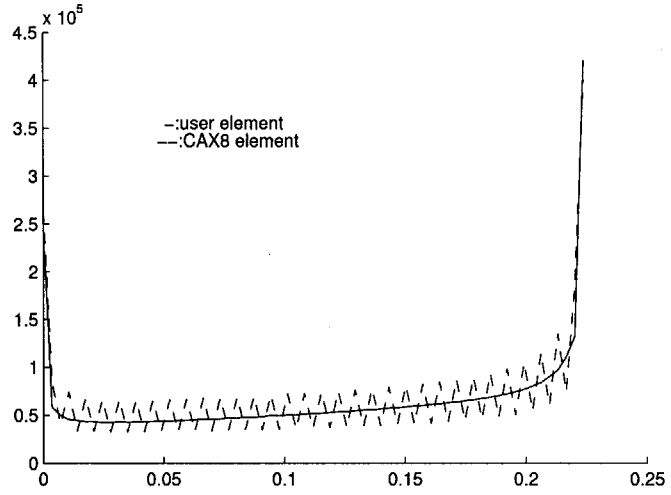

Fig. 18. Normal pressures along contact surface 2

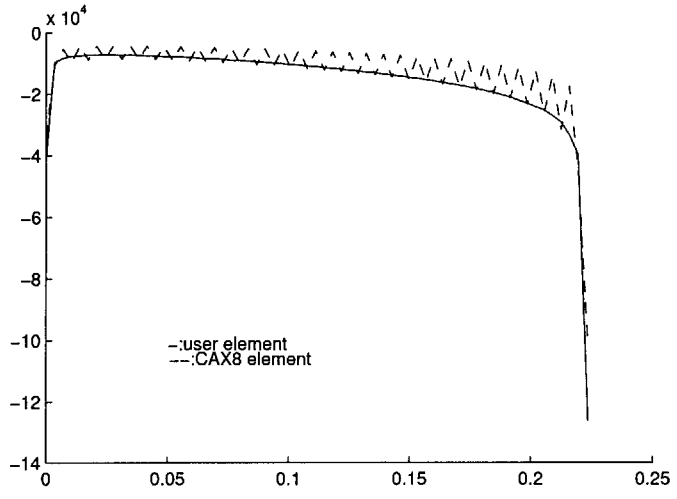

Fig. 19. Tangential shear stresses along contact surface 2

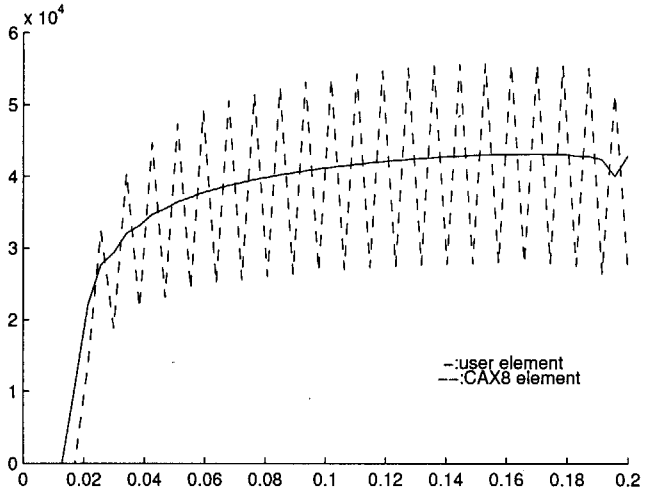

Fig. 20. Normal pressures along contact surface 3

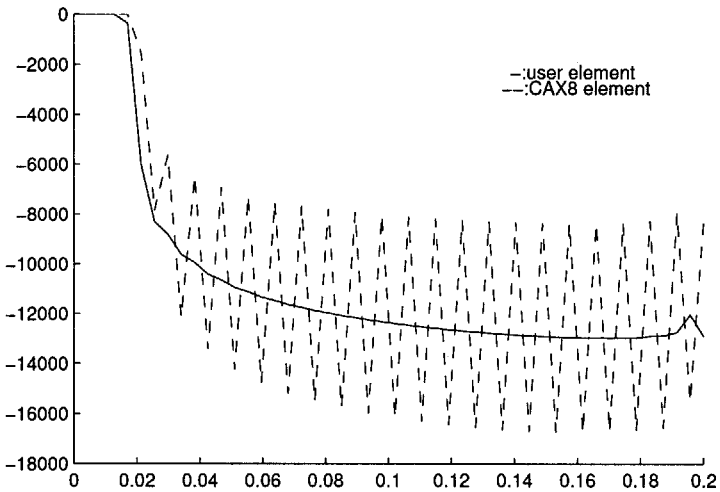

Fig. 21. Tangential shear stresses along contact surface 3

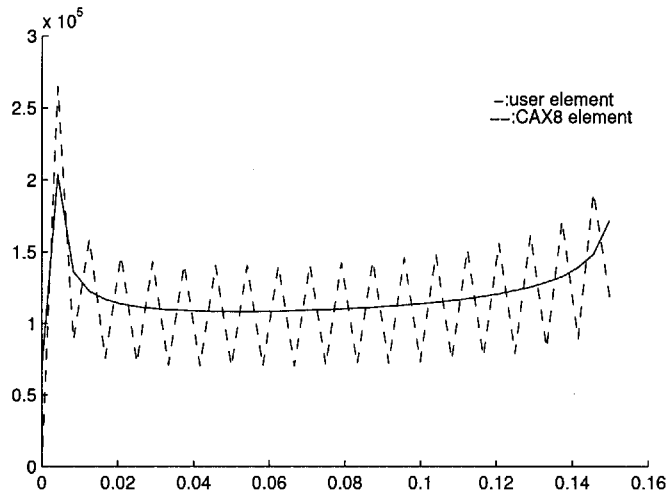

Fig. 22. Normal pressures along contact surface 4

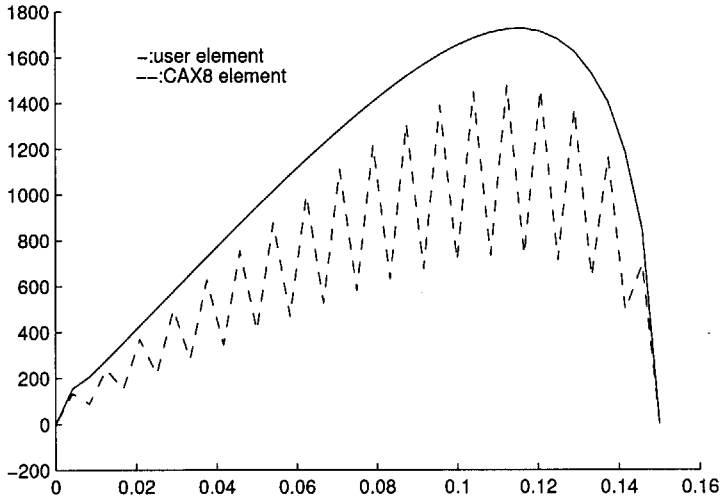

Fig. 23. Tangential shear stresses along contact surface 4

in the previous sections works quite well: the maximum difference in the first six eigenvalue between user element and standard ABAQUS elements CAX6 and CAX8 is less than 0.3%.

Table 1. The first six eigenvalues from different elements

Mode No.	1	2	3	4	5	6
CAX6	36389.	1.9319E+06	3.8114E+06	3.9787E+06	5.7680E+06	7.6025E+06
6-node user element	36386.	1.9317E+06	3.8104E+06	3.9763E+06	5.7636E+06	7.5964E+06
CAX8	36386.	1.9320E+06	3.8113E+06	3.9784E+06	5.7679E+06	7.6010E+06
8-node user element	36390.	1.9310E+06	3.8080E+06	3.9723E+06	5.7537E+06	7.5789E+06

7.6. Buckling load of a beam

This problem originates from Kleiber and Woźniak [7]. A thin simply supported beam in plane stress state is taken into consideration. This type of modelling makes it possible to analyse the in-plane deformation of the beam only. The geometry and mesh for half the beam, that allows to analyse the first mode of buckling, are given in Fig. 24. The second (antisymmetric) mode of buckling is analysed with the same mesh, but different boundary conditions as shown in Fig. 25. The thickness of the beam is 0.1 m. Young's modulus E and Poisson's ratio are $2.07 \cdot 10^{11}$ per square meter and 0 (as in the beam theory), respectively. A horizontal concentrated load P is applied at point A.

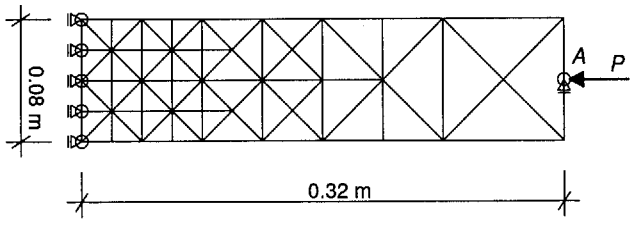

Fig. 24. Mesh and boundary conditions for symmetric in-plane buckling of a simply supported beam

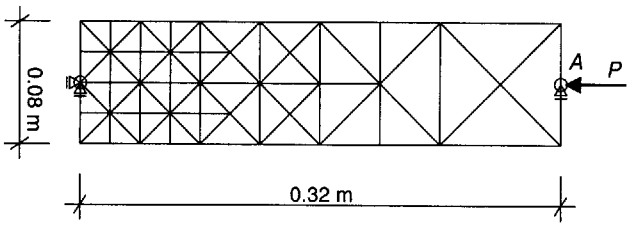

Fig. 25. Mesh and boundary conditions for antisymmetric in-plane buckling of a simply supported beam

Let us note that the classical Euler beam buckling stress is given in this case by the formula

$$\sigma_{cr} = \frac{n^2\pi^2 EI}{AL^2} \tag{27}$$

in which I is the moment of inertia, L is the length of the beam, A is the cross-sectional area and n is the mode number. For the first mode $\sigma_{cr} = 2660$ MPa, whereas for the second mode $\sigma_{cr} = 10640$ MPa. The calculated buckling stresses using ABAQUS standard element CPS6, modified element CPS6M and 6-node user element are given in Table 2.

Table 2. Critical stresses for the first and second mode using CPS6 and 6-node user element

Mode	1	2
CPS6	2.6208E+09	9.8096E+09
CPS6M	2.6105E+09	9.6683E+09
6-Node User Element	2.5608E+09	9.1833E+09

The difference from the analytical results is 3.7% and 13.7% for the first and second mode, respectively. However, notice that the critical values obtained from the new element are on the safe side, what can be advantageous in many applications.

8. Conclusions

The paper proposes a new method to establish piece-wise linear weight functions for 2-D quadratic elements: 6-node triangular element and 8-node quadrilateral element. Derivations of stiffness and mass matrices of a 6-node triangular element by using this new method are presented. The stiffness and mass matrices of an 8-node quadrilateral element are also derived by condensing two 6-node triangular elements. Numerical examples considering contact problems are given and the results are compared between different methods showing good performance of the proposed method concerning mostly 2-D contact problems.

References

[1] *ABAQUS User's Manual, Version 5.7.* Hibbitt, Karlsson & Sorensen, Inc, 1997.
[2] K. J. Bathe. *Finite Element Procedures in Engineering Analysis.* Prentice Hall, pp. 341–379, 1982.
[3] R. Buczkowski and M. Kleiber. Elasto-plastic interface model for 3D-frictional orthotropic contact problems. *Int. J. Numer. Methods Eng.*, **40**: 599–619, 1997.
[4] R. D. Cook. *Concepts and Applications of Finite Element analysis.* John Wiley & Sons, pp. 181–183, 311–315, 1981.

[5] A. Jarzębowski, J. Maciejewski. Some remarks on the applicability of rectangular elements to plane strain boundary value problems. *Computer Assisted Mechanics and Engineering Sciences*, **5**: 299–309, 1998.
[6] M. Kleiber (Ed.). *Handbook of Computational Solid Mechanics.* Springer, pp. 25–31, 1998.
[7] M. Kleiber, C. Woźniak. *Nonlinear Mechanics of Structures.* Polish Scientific Publishers, pp. 229–232, 379–380, 1991.
[8] J. T. Oden, E. B. Pires. Algorithms and numerical results for finite element approximations of contact problems with non-classical friction laws. *Computers & Structures*, **19**: 137–147, 1984.
[9] N. Ottosen and H. Petersson. *Introduction to the Finite Element Method.* Prentice Hall, pp. 142–156, 1992.
[10] T. Uchiyama. Petrov–Galerkin finite element method for gas liquid two-phase flow based on an incompressible two-fluid model. *Nuclear Engineering and Design*, **193**: 145–157, 1999.
[11] P. Wriggers, T. Vu Van and S. Stein. Finite element formulation of large deformation impact-contact problems with friction. *Computers & Structures*, **37**: 319–331, 1990.